International Journal of Engineering and Geosciences
https://dergipark.org.tr/en/pub/ijeg
e-ISSN 2548-0960

The Effect of Ground Control Points Located on Roofs on Building Facade Accuracy

Hasan Dilmac [1], Veli Ilci [*1], Tilbe Sasmaz [1], Ibrahim Murat Ozulu [2]

[1] *Ondokuz Mayis University, Faculty of Engineering, Turkiye, hasan.dilmac@omu.edu.tr, veli.ilci@omu.edu.tr, tilbe.sasmaz@gmail.com*
[2] *Hitit University, Architecture and Urban Planning, Turkiye, imuratozulu@hitit.edu.tr*

Cite this study: Dilmac, H., Ilci, V., Sasmaz, T., & Ozulu, I. M. (2024). The Effect of Ground Control Points Located on Roofs on Building Façade Accuracy. International Journal of Engineering and Geosciences, Volume (Issue), 1-9.164-172.

https://doi.org/10.26833/ijeg.1535675

Keywords
UAV
Photogrammetry
GCP
Facade
Accuracy

Research Article

Received:19.08.2024
Revised: 20.09.2024
Accepted:24.09.2024
Published:01.07.2025

Abstract

The popularity of Unmanned Aerial Vehicle (UAV) photogrammetry is growing worldwide due to its low-cost advantage in collecting high-resolution 3D topographic models. This research aims to ascertain the impact of Ground Control Points (GCPs) located on building roofs on facade accuracy. A UAV survey covering 10.37 hectares was conducted to achieve this goal. The research utilised 91 GCPs for geo-referencing, with 38 on the ground and 53 on the roofs of the buildings in the area. Images were obtained with three different flight patterns: single (S), double (D), and circular (C), which represent flight routes. The images acquired from the flights have been subjected to two distinct GCP configurations, and two models were obtained for each flight pattern. The point cloud produced by a robotic total station was used to ensure the accuracy of the facades of the buildings in the models. The standard deviation (std. dev.) of the distances between the points on the facade and the reference planes (RPs) were used as a measure of accuracy. The std. dev. values of the model facades were compared by each other while considering the number of points of the surfaces. Average std. dev. values of the models fluctuate within a range of 7 to 11 cm.

1. Introduction

Recent improvements in hardware and software have enabled the use of Unmanned Aerial Vehicles (UAVs), known as drones, for accurate 3D modeling [1-4]. With the growing use of UAVs, various software packages have been developed that enable photogrammetric or structure-from-motion (SfM) analysis [5]. Using image sensors, UAV photogrammetry can extract 3D geometric information and point clouds from overlapping photos [6, 7]. For 3D reconstruction, plenty of photogrammetric software and tools are available, both open-source and commercial [8]. Typically, these software adhere to a five-step approach to achieve 3D photogrammetric reconstruction: identifying and matching features, determining the position of points using triangulation, generating a detailed point cloud, creating a surface or mesh representation, producing a digital surface model, and generating an orthophoto [9]. Nowadays, practically every mapping project, including those in the fields of agriculture [10], forestry [11], archaeology [12-15], emergency management [16], open mine [17], road monitoring [18, 19], and shoreline detection [20], uses UAV sensors and platforms [21]. Using SfM computer-vision software and current photogrammetry concepts, UAVs can create ultra-high-resolution orthomosaics and high-density point clouds [22-25].

The accuracy and quality of the outputs obtained by UAV photogrammetry are crucial for many types of research like mapping, 3D modeling, and so on [26]. Positional correctness refers to the degree of proximity between these values and the object's actual position. The desired level of positional accuracy varies depending on the requirements of the study [27]. It's evident from the literature that some photogrammetric parameters (GCP, altitude, etc.) affect the model's accuracy [28-31]. Those that have the most significant impact on the output's correctness include image overlap. This photogrammetric quantity expresses how much overlap exists between two parallel images and Ground Control

Points (GCPs), which are usually deployed as part of UAV mapping to georeference the images and topographic model [32]. For 3D modeling, a specific quantity of side and front overlap in images is needed. The overlap percentages will determine the number of flight lines, the number of images taken, and the interval between shots. In addition, flight patterns affect the number of images captured. Various flying patterns, such as single (S), double (D), and circular (C), can be generated depending on the necessary data and the dimensions of the research area [33].

GCPs are an essential part of the overall survey activity and play an important part in the procedure required to obtain accurate georeferenced positional data from UAV photogrammetry [34]. Because the accuracy of photogrammetric outputs is directly impacted by the GCPs used [35], numerous researchers have carried out a range of studies over the years to assess the accuracy of UAV products by varying their quantity and position of GCPs [36]. [37] analysed the effect of the number of GCPs on the accuracy of UAV-photogrammetry outputs by using 72 points as GCPs and control points (CPs). Taking into account 4, 5, 6, 7, 8, 9, 10, 15, and 20 GCPS, they made five replications of photogrammetric projects in which the distribution of GCPs was changing. The number of CPs ranged from 52 to 69, depending on the number of GCPs utilised. They used RMSE values to analyse the accuracy of 45 projects in total. RMSE values were calculated using the GPS coordinates and orthoimage coordinates of CPs. They reached lower RMSE values for 15 and 20 GCPs. Their study suggests that horizontal and vertical accuracy increases as the number of GCPs increases. [38] investigated whether the 1:20, 1:50, 1:100, and 1:200 scale accuracy requirements were met by the DJI Phantom 4 RTK drone. To do this, they chose a building with four facades and placed 109 signalised points (SP) on each facade, whose coordinates were measured with a total station. They collected images for each facade in both RTK and NRTK modes with manual flight. For evaluation, they adopted the Single-Façade (S-F) approach, in which each facade is considered separately, and the 4-Façade (4-F) approach, in which the four facades are evaluated together. During the evaluation phase, they applied three different strategies: (1) no GCP, (2) one GCP close to the building, and (3) one SP on each facade as GCP. They observed that with the S-F approach, metric standards for the 1:50 scale were met without using GCP, but for the 4-F approach, strategy (3) had to be used. They also concluded that the best results were achieved with this strategy. [39] tested the impact of different GCP distributions on the accuracy of spatial data obtained from UAV photogrammetry according to four configurations. He used a total of 21 GCPs (measured by RTK GPS) as control points and checkpoints for georeferencing and accuracy assessment. Four GCPs were on the roof of the building and the remaining were fixed and distributed within the garden and parking areas. In four different configurations, while the number of control points varied between 3 and 7, the remaining points were used as checkpoints to assess spatial accuracy. The best horizontal and vertical accuracy was achieved in the configuration where 7 GCPs (one in the centre and the rest at boundaries) were utilised for geo-referencing, and RMSE values ranged between 0,04 and 0,06 m.

In addition to the studies above, much research has been conducted to investigate UAV accuracy in relation to the quantity and distribution of GCPs [29]. Nevertheless, these studies evaluate accuracy generally point-by-point, based on the discrepancy between the UAV and GPS coordinates of GCPs that are not utilised for georeferencing [40-42]. Moreover, vertical evaluation is generally executed through GCPs located on the horizontal plane, not on the vertical plane like building facades. But, facade models of buildings have a crucial role in many studies, such as urban planning, disaster management, sustainable development research, solar radiation estimations, etc [43,45]. Thus, having accurate information on building facades and accurate analysis of them according to GCPs would be beneficial.

This study aims to ascertain how GCPs positioned on building roofs affect facade accuracy. To accomplish this task, a UAV survey was conducted in an area of 10.7 ha. The geo-referencing process involved 91 GCPs, with 38 on the ground and 53 on the roofs of two buildings. S, D, and C flight patterns were adopted, and the images obtained from autonomous flights were processed twice by using 38 GCPs (only GCPs on the ground) and 91 GCPs to determine whether the 53 GCPs placed on building roofs would improve the facade accuracy of buildings. In order to conduct a comparative analysis, reference point cloud data of the buildings was gathered using a robotic total station, ensuring that the data had a sufficient number of points. Joint surfaces chosen over the buildings were used to calculate the standard deviation (std. dev.) of the distances between model points and reference planes generated from the reference point cloud.

2. Material and Method

2.1. Study area

The study area is located in Samsun, a city in northern Türkiye, and spans 10,37 hectares on the campus of Ondokuz Mayis University. The region has a wide variety of topographical features, including buildings, roads, sidewalks, and vegetated areas. The three-dimensional (3D) models of Engineering Faculty buildings within the region are the main interest of this study. The engineering faculty consists of two buildings: the main building with six floors and the outbuilding with two floors (Figure 1).

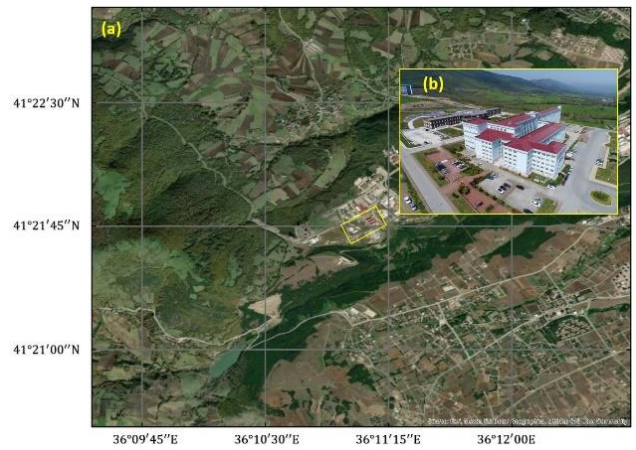

Figure 1. Study area (a: location map, b: the buildings)

2.2. Ground control points (GCPs)

To georeference the point clouds generated from UAV images to a global coordinate system, three groups of GCPs surveyed using global navigation satellite system (GNSS) techniques were utilised (Figure 2). For the first GCP group, composed of 11 points, four hours of static GNSS observations were carried out using multi-frequency Topcon HiperPro GNSS receivers.

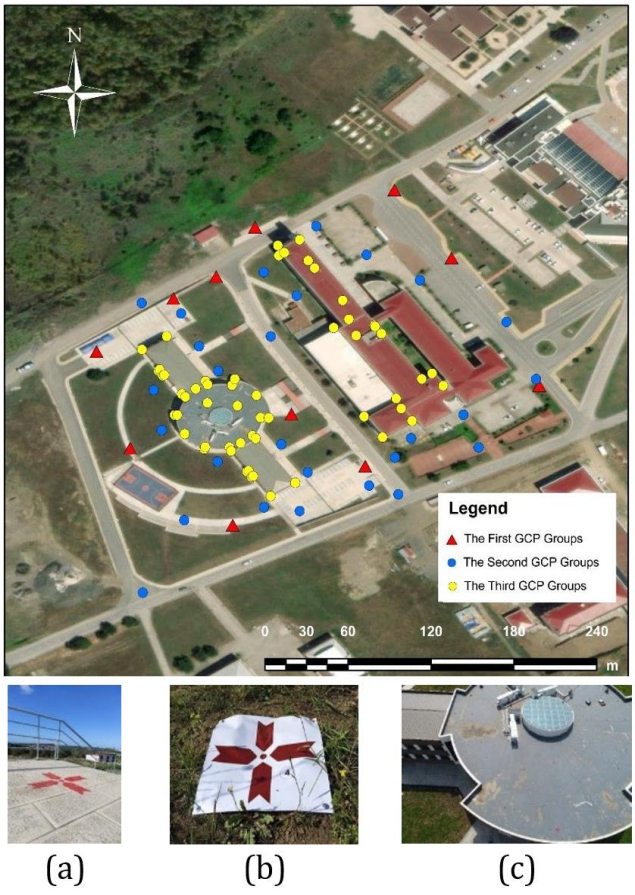

Figure 2. GCPs (a: static measurement points that are red triangle points, b: RTK measurement points on the ground that are blue circle points in the figure, c: RTK measurement points at the top and top corner of the buildings that are yellow circle points)

The static data from continuously operating reference stations at 1-second intervals is used to guide static processes. One of these points is a concrete pillar, and 10 of these points were marked to the ground with a huge metal screw, and to ensure visibility in the images, they were painted red (Figure 2a). The second GCP group consists of 27 temporal points marked on the ground using vinyl (Figure 2b). The third GCP group consists of 53 points painted red on the top and top corners of the buildings (Figure 2c). The second and third GCP groups were surveyed using Network Real Time Kinematic (NRTK) techniques. GCPs were projected onto the UTM zone 36N coordinate system in the datum of the ITRF96 2005.0 epoch.

2.3. Ground control points (GCPs)

The DJI Phantom 4 Pro was used to collect data with a 20-megapixel CMOS sensor, measuring one inch, with a f2.8–/f11 wide-angle lens with an equivalent focal length of 24 mm. The study area was flown by three flight patterns: Single (S), Double (D), and Circular (C) (Figure 3).

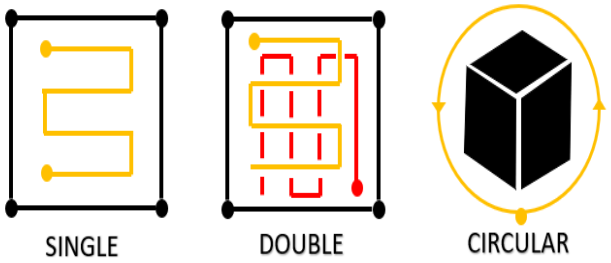

Figure 3. Flight patterns

The UAV flew autonomously, following a preconfigured route on each flight. In the S pattern, forward and side overlaps were fixed at 80% and 70%, respectively. The flight altitude was constant above ground level, resulting in an average ground sampling distance (GSD) of 1.59 cm/pixel. One flight was enough to cover the study area, and a total of 244 images were obtained after a flight of 14 minutes. The D pattern overlaps the same forward and side with the S pattern. A total of 1056 images with an average GSD of 1.24 cm/pixel were taken during four flights lasting 60 minutes in total. In the C pattern, two flights, each lasting eight minutes, were flown around two Engineering Faculty buildings. The side overlap was fixed at 90% for both buildings, and a total of 295 images of the scene were obtained.

Pix4Dmapper software was utilised to conduct the photogrammetric process. The software's accuracy has been proven to be satisfactory in many studies [9, 44]. To evaluate the effect of GCPs positioned on roofs, each flight was processed with two GCP configurations, thus making a total of six models (Table 1).

Table 1. Process parameters and results

Flight Pattern	Number of GCPs	RMSE (cm)	Number of Points in the Clouds
S	38	5	154,959,527
	91	2.9	148,203,420
D	38	2.4	113,866,660
	91	1.9	115,806,788
C	38	3.5	23,905,969
	91	2.8	25,158,098

2.4. Reference point cloud

A highly sensitive TS16 robotic total station was used to gather the reference point cloud, which was then used to assess the facade accuracy of the generated models. Eleven GCPs acquired through the static measurements shown in Figure 2 were utilized for this purpose. This device, which can automatically scan the grid between selected points and with specified vertical and horizontal angle ranges, has a non-prism measurement range of 1-1000 m and a precision of 2 mm + 2 ppm with a minimum angle reading of 0.3 mgon. After choosing 0.2 gon for the horizontal and 0.5 gon for the vertical grid scanning intervals, a reference point cloud with 157,916 points was produced (Figure 4).

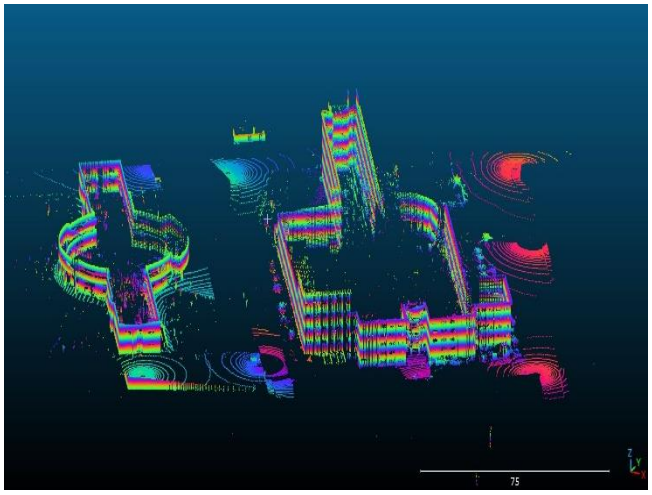

Figure 4. Reference point cloud

2.5. Accuracy evaluation method

For the accuracy analysis of the facades in the produced models (which we will refer to as Model Facade – MF), the std. dev. values of the distances between the points in MF and reference planes (RP) were calculated. Nine facades (F1 – F9) on buildings were determined to be used for comparison while guaranteeing that facades were from all directions and that these facades had enough points to form an RP (Figure 5).

Figure 5. The facades chosen for the accuracy assessment of the models

RPs were generated in two steps using the Cloud Compare v2.12.4 software. First, the segmentation step (Figure 6a), in which the extraction of facades from the reference point cloud was performed, followed by the step of fitting a plane to the points in the extracted facades (Figure 6b).

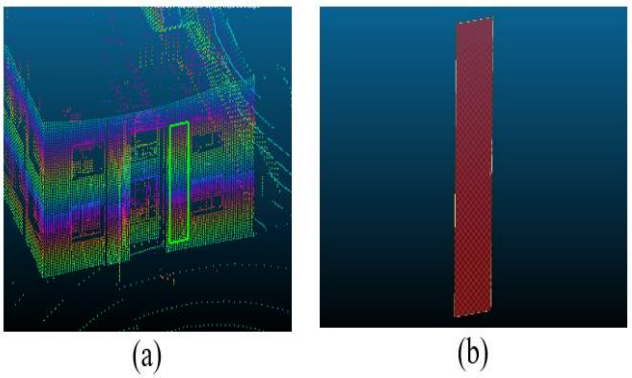

Figure 6. Reference planes. 6a: the segmentation step 6b: plane fitting step

The same segmentation step was performed with the models to produce MFs. Then, the std. dev. value of the distances between the points of MFs and RPs was computed according to equation (1):

$$std.dev. = \sqrt{\frac{1}{n}\sum_{i=1}^{n}(d_i - d_{mean})^2} \quad (1)$$

Here, n is the number of points in the MFs, d_{mean} is the mean of the distances, d_i is the distance between the model points and reference plane (Figure 7).

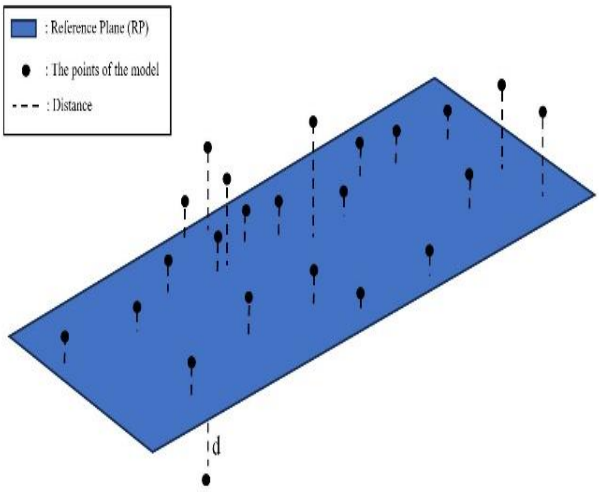

Figure 7. The computation of the point/plane distance

3. Results and Discussion

The steps discussed in the previous section were carried out, and nine std. dev. values for each model (a total of 9 facades x 6 models = 54 std. dev.) were obtained for the facades of each model (Figure 8). There is conflicting evidence regarding whether GCPs installed on roofs increase the model facade's accuracy. In the D pattern, while the model with 91 GCPs generated more accurate results for F1, F2, F3, F7, and F9, the model with 38 GCPs generated more accurate results for F4, F5, and F8. There is a similar situation between the models of the C pattern.

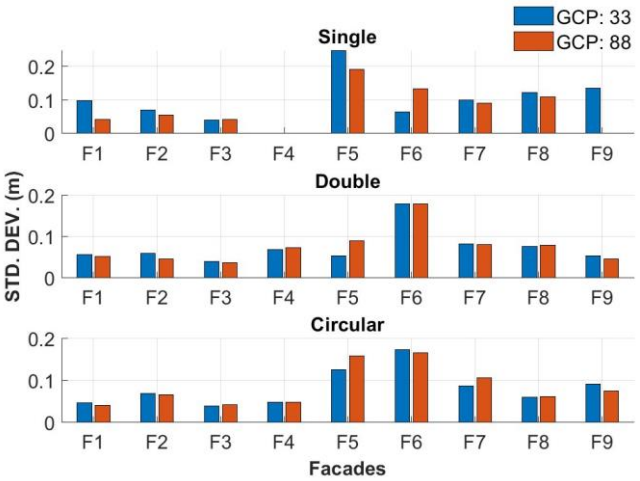

Figure 8. The std. dev. values of each facade for three patterns (S, D, and C) with varying GCP configuration

When std. dev. values for each facade are taken into account, F6 earned the poorest std. dev. values with a significant difference. It is because the UAV's camera view angle was severely restricted due to its proximity to the flight boundaries in the area where F6 exists. The average std. dev. values of each pattern are changing in the 7-11 cm range. In the S pattern, the std. dev. of the model obtained using 91 GCPs is lower than the model values obtained using 38 GCPs, except for the F3 and F6. The modest std. dev. values were acquired for F5 in both models of the S pattern. Although it has been observed that placing the GCPs on the roof reduces the std. dev. values in the S pattern, the results obtained with the S pattern will be ignored for this study because they didn't have enough points (even no data for some facades) that can define a plane (Figure 9). In the D pattern, both models (the D pattern with 38 GCPs and the D pattern with 91 GCPs) delivered identical std. dev. values for the majority of the facades, and their std. dev. means are 7 and 8 cm, respectively. Therefore, unlike the S pattern, the placement of GCPs on rooftops did not reduce the std. dev. values in the D pattern. Both D pattern models (with 38 GCPs and 91 GCPs) have enough points to define a plane in the facades except F6 and F7 (Figure 10). As for the C pattern, the models have identical results, just as in the D pattern. The average std. dev. values of C pattern models (with 38 GCPs and 91 GCPs) are 8 cm and produce enough points to define a plane in the facades, even for F6, unlike the S and D patterns (Figure 11).

In many studies, how the number and distribution of GCPs affect the accuracy of UAV photogrammetry outputs is investigated by testing different combinations. The GCPs are typically placed at the corners or center and their numbers are incrementally increased to test the accuracy of UAV outputs. These tests use RMSE values between the GNSS coordinates, which are assumed to be more accurate, and the model coordinates of the GCPs which were not used in the geo-referencing process [42]. [41] stated that RMSE values improve incrementally up to a certain number of GCPs and that for the best results, GCPs should be uniformly distributed, with at least one GCP positioned near the center. In their study, [36] conducted geo-referencing using three different

scenarios, starting with 4 GCPs and increasing the number to 35. In the first scenario, the GCPs were distributed at the corners, in the second, they were centrally distributed, and in the third, they were uniformly distributed. To compare the accuracy of the resulting models, 30 CPs were used. The best horizontal accuracy was found in the first scenario with $RMSE_{xy}$: 0.033 m, and the best vertical accuracy was achieved in the third scenario with $RMSE_z$: 0.048 m. However, in these studies, model accuracy is assessed by comparing the model coordinates with GNSS coordinates using a relatively small number of CPs. While this is an important criterion for evaluating model accuracy at specific points, it provides limited information about the overall accuracy of surfaces with thousands of points, which include various components like buildings, trees, roads, and sidewalks. It is well-known that models obtained through UAV photogrammetry can contain noisy point data. For this reason, in our study, the accuracy analysis was conducted using all the points on the selected surfaces, and the results were expressed as the standard deviation of the distances from these points to the reference surfaces.

One of the purposes of producing 3D models is to enable the modeling of buildings in the study area. Buildings are complex structures composed of various components, such as floors and facades. Therefore, conducting accuracy analyses based on CPs placed in areas unrelated to the building does not provide complete information about the accuracy of these buildings. In this study, accuracy analyses were specifically performed on building facades. Additionally, the impact of placing GCPs on rooftops on the accuracy of the building facades was also investigated.

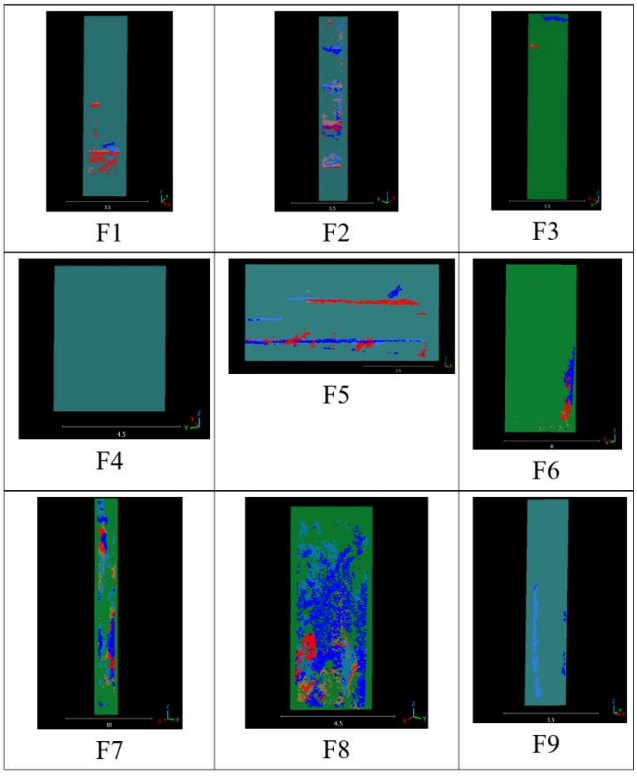

Figure 9. The point distribution and number of S patterns in each facade. The blue points demonstrate the S model acquired using 38 GCPs, and the red ones demonstrate the S model obtained using 91 GCPs

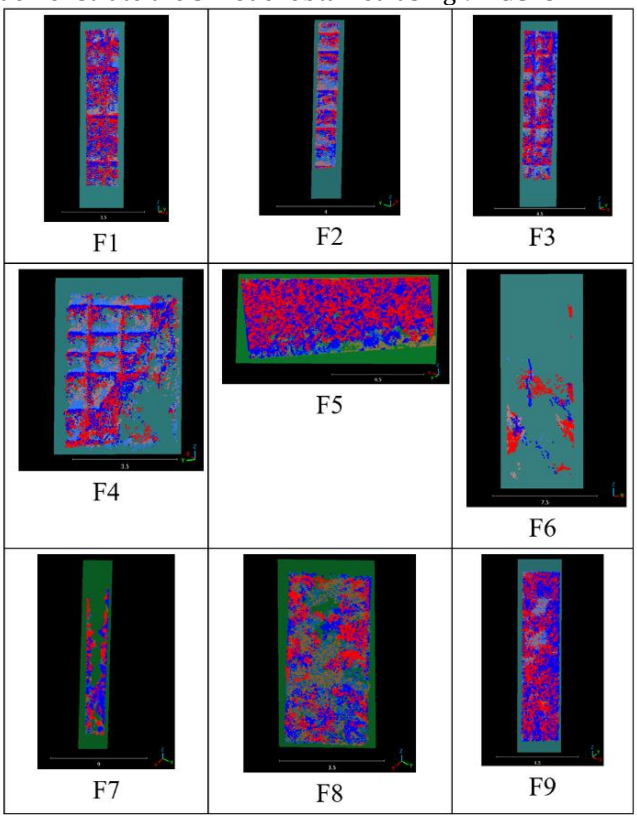

Figure 10. The point distribution and number of D patterns in each facade. The blue points demonstrate the D model acquired using 38 GCPs, and the red ones demonstrate the D model obtained using 91 GCPs

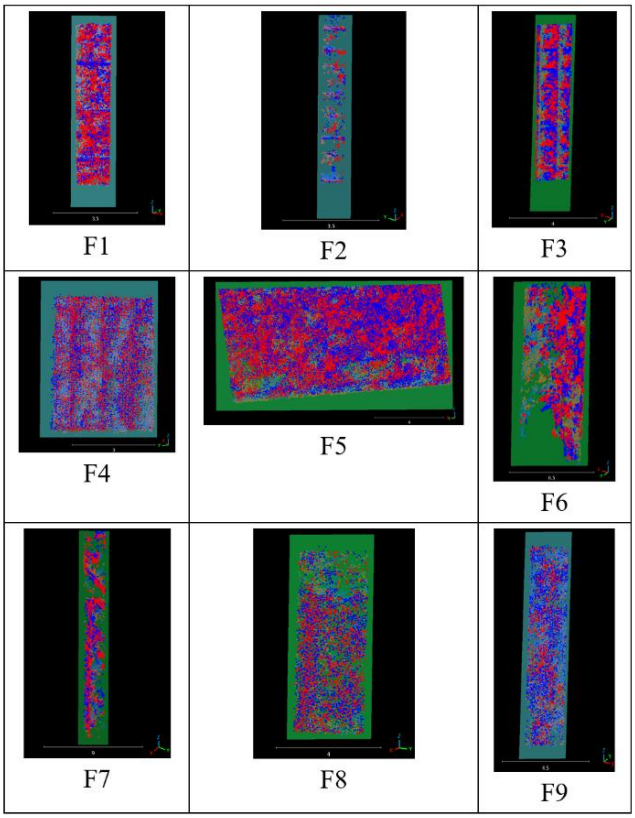

Figure 11. The point distribution and number of C patterns in each facade. The blue points demonstrate the C model acquired using 38 GCPs, and the red ones demonstrate the C model acquired using 91 GCPs

4. Conclusion

One of the newest mapping methods, UAV photogrammetry, provides high-resolution landscape data in a digital context. Researchers in earth sciences are particularly interested in its use for small-scale area surveys. The quantity and variety of GCPs can significantly impact the accuracy of the spatial data obtained from UAV photogrammetry. In prior research in the photogrammetric literature, the number of GCPs to employ in a standard aerial manned survey was examined. It's common knowledge that increased use of control points improves accuracy. For UAV-based photogrammetry, these guidelines need to be applicable at first. However, achieving enough accuracy while minimising operating costs necessitates a compromise due to the high expenses associated with setting up GCPs over vast geographic areas.

In this study, two different GCP configurations have been applied to the images obtained from three flights to analyse the effect of GCPs placed on the building's roofs on facade accuracy. Two models were generated from each flight by using 38 GCPs (only GCPs on the ground) and 91 GCPs (including 53 GCPs on the roofs). In the S pattern, GCPs on the roof improved accuracy by up to 6 cm on some facades. However, both models of the S pattern do not have enough points to determine a plane in these facades. Thus, they bear no meaningful results about the effect of GCPs on facade accuracy for this study. Moreover, the results of D and C patterns show that if the 1 cm improvement is not important for the goal of the study, installing GCP on roofs would be a waste of time and effort.

Author contributions

Hasan Dilmac: Conceptualization, Methodology, Software, Field study, Original draft preparation **Veli İlci:** Data curation, Software, Validation., Field study **Tilbe Sasmaz:** Visualization, Investigation, Writing-Reviewing and Editing **İbrahim Murat Ozulu:** Visualization, Investigation, Writing-Reviewing and Editing.

Conflicts of interest

The authors declare no conflicts of interest.

References

1. Ajayi, O. G., Palmer, M., & Salubi, A. A. (2018). Modelling farmland topography for suitable site selection of dam construction using unmanned aerial vehicle (UAV) photogrammetry. Remote Sensing Applications: Society and Environment, 11, 220-230. https://doi.org/10.1016/j.rsase.2018.07.007
2. Szypuła, B. (2024). Accuracy of UAV-based DEMs without ground control points. Geoinformatica, 28(1), 1-28. https://doi.org/10.1007/s10707-023-00498-1
3. Sefercik, U. G., Kavzoglu, T., Colkesen, İ., Nazar, M., Ozturk, M. Y., Adalı, S., & Din, S. (2023). 3D positioning accuracy and land cover classification performance of multispectral RTK UAVs. International Journal of Engineering and Geosciences. 8(2), 119-128. https://doi.org/10.26833/ijeg.1074791
4. Karataş, L., Alptekin, A. & Yakar, M. (2022). Creating Architectural Surveys of Traditional Buildings with the Help of Terrestrial Laser Scanning Method (TLS) and Orthophotos: Historical Diyarbakır Sur Mansion. Advanced LiDAR, 2(2), 54-63.
5. Murtiyoso, A., Grussenmeyer, P., Börlin, N., Vandermeerschen, J., & Freville, T. (2018). Open source and independent methods for bundle adjustment assessment in close-range UAV photogrammetry. Drones. 2(1), 1–18. https://doi.org/10.3390/drones2010003
6. Colica, E., D'Amico, S., Lannuci, R., Martino, S., Gauci, A., Galone, L., Galea, P., & Paciello, A. (2021). Using unmanned aerial vehicle photogrammetry for digital geological surveys: case study of Selmun promontory, northern of Malta. Environmental Earth Sciences, 80(17), 1–14. https://doi.org/10.1007/s12665-021-09846-6
7. Maraş, E. E., & Nasery, M. N. (2023). Investigating the length, area and volume measurement accuracy of UAV-Based oblique photogrammetry models produced with and without ground control points. International Journal of Engineering and Geosciences. 8(1), 32–51. https://doi.org/10.26833/ijeg.1017176
8. Đurić, I., Vasiljević, I., Obradović, M., Stojaković, V., Kićanović, J., & Obradović, R. (2021). Comparative analysis of open-source and commercial photogrammetry software for cultural heritage. eCAADe 2021 Towards a New, Configurable Architecture, 2, 8-10, Novi Sad, Serbia.
9. Jarahizadeh, S., & Salehi, B. (2024). A Comparative Analysis of UAV Photogrammetric Software Performance for Forest 3D Modeling: A Case Study Using Agisoft Photoscan, PIX4DMapper, and DJI Terra. Sensors, 24(286), 1–15. https://doi.org/10.3390/s24010286
10. Janoušek, J., Jambor, V., Marcoň, P., Dohnal, P., Synková, P., & Fiala, P. (2021). Using UAV-based photogrammetry to obtain correlation between the vegetation indices and chemical analysis of agricultural crops. Remote Sensing, 13(10), 1878. doi: 10.3390/rs13101878.
11. Frey, J., Kovach, K., Stemmler, S., & Koch, B. (2018). UAV photogrammetry of forests as a vulnerable process. A sensitivity analysis for a structure from motion RGB-image pipeline. Remote Sensing, 10(912),1–12. https://doi.org/10.3390/rs10060912
12. İlci, V., & Ozulu, İ. M. (2016). The Utility of PPP Technique in Archaeological Surveying Applications: A Case Study in Sapinuva Excavation. Harita Teknolojileri Elektronik Dergisi, 8(3), 1-9. doi: 10.15659/hartek.16.09.303.
13. Kanun, E., Alptekin, A., & Yakar, M. (2021). Cultural heritage modelling using UAV photogrammetric methods: a case study of Kanlıdivane archeological site. Advanced UAV, 1(1), 24–33.
14. Yakar, M., Yılmaz, H. M. & Mutluoğlu, Ö. (2010). Comparative evaluation of excavation volume by TLS and total topographic station-based methods. Lasers in Eng, 19, 331-345

15. Özdemir, İ., & Güngör, A. (2024). Documentation of Archaeological Excavation Sites with Terrestrial Laser Scanning and UAV Photogrammetry Methods. Advanced LiDAR, 4(1), 28-32.
16. Mandirola, M., Casarotti, C., Peloso, S., Lanese, I., Brunesi, E., Senaldi, I., Monti, A., & Facchetti, C. (2021). Guidelines for the use of Unmanned Aerial Systems for fast photogrammetry-oriented mapping in emergency response scenarios. International Journal of Disaster Risk Reduction, 58(102207), 1-15. https://doi.org/10.1016/j.ijdrr.2021.102207.
17. Erdoğan, A., Görken, M., & Kabadayı, A. (2022). Study on the use of unmanned aerial vehicles in open mine sites: A case study of Ordu Province Mine Site. Advanced UAV, 2(2), 35-40.
18. Douglas, A., Langenderfer, A. M., & Johnson, C. (2024). Road Condition Monitoring Utilizing UAV Photogrammetry Aligned to Principal Curve of Mine Haul Truck Path. Mining, Metallurgy & Exploration, 41, 61-72. https://doi.org/10.1007/s42461-023-00877-0
19. Polat, N., & Akça, Ş. (2023). Assessing road roughness using UAV-derived dense point clouds. Mersin Photogrammetry Journal, 5(2), 75-81. https://doi.org/10.53093/mephoj.1358902
20. Aykut, N. O. (2019). İnsansız hava araçlarının kıyı çizgisinin belirlenmesinde kullanılabilirliğinin araştırılması. Geomatik, 4(2), 141-146. https://doi.org/10.29128/geomatik.503055
21. Budiharto, W., Irwansyah, E., Suroso, J. S., Chowanda, A., Ngarianto, H., & Gunawan, A. A. S. (2021). Mapping and 3D modelling using quadrotor drone and GIS software. Journal of Big Data, 8(1), 1-12. https://doi.org/10.1186/s40537-021-00436-8
22. Sona, G., Pinto, L., Pagliari, D., Passoni, D., & Gini, R. (2014). Experimental analysis of different software packages for orientation and digital surface modelling from UAV images. Earth Science Informatics, 7(2), 97–107.https://doi.org/10.1007/s12145-013-0142-2
23. Lovitt, J., Rahman, M. M., & McDermid, G. J. (2017). Assessing the value of UAV photogrammetry for characterizing terrain in complex peatlands. Remote Sensing, 9(7), 715. https://doi.org/10.3390/rs9070715
24. Pathak, S., Acharya, S., Bk, S., Karn, G., Thapa, U. (2024). UAV-based topographical mapping and accuracy assessment of orthophoto using GCP. Mersin Photogrammetry Journal, 6(1), 1-8. https://doi.org/10.53093/mephoj.1350426
25. Yakar, M., Yilmaz, H. M. & Mutluoglu, O. (2010). Close range photogrammetry and robotic total station in volume calculation. International Journal of the Physical Sciences. 5(2), 086-096
26. Türk, T., Tunalioglu, N., Erdogan, B., Ocalan, T., & Gurturk, M. (2022). Accuracy assessment of UAV-post-processing kinematic (PPK) and UAV-traditional (with ground control points) georeferencing methods. Environmental Monitoring and Assessment, 194, 476. https://doi.org/10.1007/s10661-022-10170-0
27. Jiménez-Jiménez, S. I., Ojeda-Bustamante, W., Marcial-Pablo, M. D. J., & Enciso, J. (2021). Digital terrain models generated with low-cost UAV photogrammetry: Methodology and accuracy. ISPRS International Journal of Geo-Information, 10(5), 285. https://doi.org/10.3390/ijgi10050285
28. Mesas-Carrascosa, F. J., García, M. D. N., De Larriva, J. E. M., & García-Ferrer, A. (2016). An analysis of the influence of flight parameters in the generation of unmanned aerial vehicle (UAV) orthomosaicks to survey archaeological areas. Sensors, 16(11), 1-12. https://doi.org/10.3390/s16111838
29. Sanz-Ablanedo, E., Chandler, J. H., Rodríguez-Pérez, J. R., & Ordóñez, C. (2018). Accuracy of Unmanned Aerial Vehicle (UAV) and SfM photogrammetry survey as a function of the number and location of ground control points used. Remote Sensing, 10(10), 1-19. https://doi.org/10.3390/rs10101606
30. Akay, S. S., Ozcan, O., Şanlı, F. B., Bayram, B., & Gorum, T. (2021). Assessing the spatial accuracy of UAV-derived products based on variation of flight altitudes. Turkish Journal of Engineering, 5(1), 35-40.
31. Deliry, S. I., & Avdan, U. (2024). Accuracy assessment of UAS photogrammetry and structure from motion in surveying and mapping. International Journal of Engineering and Geosciences, 9(2), 165-190. https://doi.org/10.26833/ijeg.1366146
32. Barba, S., Barbarella, M., Di Benedetto, A., Fiani, M., Gujski, L., & Limongiello, M. (2019). Accuracy assessment of 3d photogrammetric models from an unmanned aerial vehicle. Drones, 3(4), 1–19. https://doi.org/10.3390/drones3040079
33. Chaudhry, M. H., Ahmad, A., & Gulzar, Q. (2020). Impact of uav surveying parameters on mixed urban landuse surface modelling. ISPRS International Journal of Geo-Information, 9(11), 1-17. https://doi.org/10.3390/ijgi9110656
34. Rangel, J. M. G., Gonçalves, G. R., & Pérez, J. A. (2018). The impact of number and spatial distribution of GCPs on the positional accuracy of geospatial products derived from low-cost UASs. International Journal of Remote Sensing, 39(21), 7154–7171. https://doi.org/10.1080/01431161.2018.1515508
35. Dharshan Shylesh, D. S., Manikandan, N., Sivasankar, S., Surendran, D., Jaganathan, R., & Mohan, G. (2023). Influence of quantity, quality, horizontal and vertical distribution of ground control points on the positional accuracy of UAV survey. Applied Geomatics, 15(4), 897–917. https://doi.org/10.1007/s12518-023-00531-w
36. Yakar, M., & Dogan, Y. (2019). 3D Reconstruction of Residential Areas with SfM Photogrammetry. In Advances in Remote Sensing and Geo Informatics Applications: Proceedings of the 1st Springer Conference of the Arabian Journal of Geosciences (CAJG-1), Tunisia 2018 (pp. 73-75). Springer International Publishing.
37. Agüera-Vega, F., Carvajal-Ramírez, F., & Martínez-Carricondo, P. (2017). Assessment of photogrammetric mapping accuracy based on variation ground control points number using unmanned aerial vehicle. Measurement, 98, 221-227.

https://doi.org/10.1016/j.measurement.2016.12.002.
38. Taddia, Y., González-García, L., Zambello, E., & Pellegrinelli, A. (2020). Quality assessment of photogrammetric models for façade and building reconstruction using dji phantom 4 rtk. Remote Sensing, 12(19), 1–32. https://doi.org/10.3390/rs12193144
39. Elkhrachy, I. (2021). Accuracy Assessment of Low-Cost Unmanned Aerial Vehicle (UAV) Photogrammetry. Alexandria Engineering Journal, 60(6), 5579–5590. https://doi.org/10.1016/j.aej.2021.04.011
40. Ferrer-González, E., Agüera-Vega, F., Carvajal-Ramírez, F., & Martínez-Carricondo, P. (2020). UAV photogrammetry accuracy assessment for corridor mapping based on the number and distribution of ground control points. Remote Sensing, 12(15), 1-19. https://doi.org/10.3390/rs12152447
41. Liu, X., Lian, X., Yang, W., Wang, F., Han, Y., & Zhang, Y. (2022). Accuracy Assessment of a UAV Direct Georeferencing Method and Impact of the Configuration of Ground Control Points. Drones, 6(2), 1-15. https://doi.org/10.3390/drones6020030
42. Martínez-Carricondo, P., Agüera-Vega, F., Carvajal-Ramírez, F., Mesas-Carrascosa, F. J., García-Ferrer, A., & Pérez-Porras, F. J. (2018). Assessment of UAV-photogrammetric mapping accuracy based on variation of ground control points. International Journal of Applied Earth Observation and Geoinformation, 72, 1–10. https://doi.org/10.1016/j.jag.2018.05.015
43. Zhang, Y., Zhang, C., Chen, S., & Chen, X. (2021). Automatic Reconstruction of Building Façade Model from Photogrammetric Mesh Model. Remote Sensing, 13(19), 3801. https://doi.org/10.3390/rs13193801
44. Jeon, E. I., Yu, S. J., Seok, H. W., Kang, S. J., Lee, K. Y., & Kwon, O. S. (2017). Comparative evaluation of commercial softwares in UAV imagery for cultural heritage recording: case study for traditional building in South Korea. Spatial Information Research, 25(5), 701–712. https://doi.org/10.1007/s41324-017-0137-z
45. Yilmaz, H. M. & Yakar, M. (2008). Computing Of Volume Of Excavation Areas By Digıtal Close Range Photogrammetry. Arabian J. Sci. Eng. 33(1A), 63-784

© Author(s) 2024. This work is distributed under https://creativecommons.org/licenses/by-sa/4.0/